IEEE Access
Multidisciplinary | Rapid Review | Open Access Journal

Received October 28, 2018, accepted December 15, 2018, date of publication January 23, 2019, date of current version February 27, 2019.

Digital Object Identifier 10.1109/ACCESS.2019.2894338

Impedance-Sum Stability Criterion for Power Electronic Systems With Two Converters/Sources

QING-CHANG ZHONG[1,2], (Fellow, IEEE), AND XIN ZHANG[3], (Member, IEEE)
[1]Department of Electrical and Computer Engineering, Illinois Institute of Technology, Chicago, IL 60616, USA
[2]SYNDEM, LLC, Chicago, IL 60616, USA
[3]School of Electrical and Electronic Engineering, Nanyang Technological University, Singapore 639798

Corresponding author: Qing-Chang Zhong (zhongqc@ieee.org)

ABSTRACT The impedance-ratio criterion is widely adopted for analyzing the small-signal stability of systems with cascaded power electronic converters. However, the impedance ratio is formed differently for different cascaded systems. In this paper, a generic impedance-sum criterion is proposed for the stability of general power electronic systems with two converters/sources. The two converters/sources can be in parallel operation, such as parallel-operated voltage-controlled inverter systems in microgrids and parallel-operated current-controlled inverter systems, or in series (cascaded) operation, such as cascaded DC/DC converter systems and grid-connected current-controlled converters. In this paper, it is shown at first that in order for a converter/source to be stable both the impedance and its inverse should be stable, that is, the impedance should not have any right-half-plane (RHP) zeros or RHP poles. Then, it is shown that a system with two individually stable converters/sources is stable if and only if the sum of the individual impedances does not have any RHP zeros or, equivalently, the impedance sum does not encircle the origin clockwise. This generic criterion is then demonstrated via applications covering all four possible cases.

INDEX TERMS Power electronic systems with two converters/sources, cascaded systems, parallel-operated system, impedance-ratio criterion, generic stability criterion, impedance-sum criterion.

I. INTRODUCTION

Power electronic systems are nowadays widely used in space stations, shipboards, and hybrid vehicles etc., thanks to their flexible configurations, high efficiency, and high density [1]–[3]. Many power electronic converters are also being used in modern power systems, accelerating the paradigm change of power systems into power electronics-enabled synchronized and democratized (SYNDEM) smart grid [4], [5]. Because of the interaction between subsystems, these systems with multiple power electronic converters may become unstable even if individual converters are stable alone. This has become a serious concern [6]–[9].

The stability of power electronic systems has been widely studied in the literature, e.g. covering constant power loads [10]–[16], constant power generators [17], [18], phase-locked loops [19]–[21], droop-controlled converters [22]–[24], and harmonics [25]–[28]. However, no *generic* stability criteria are available yet.

For cascaded power electronic systems, the impedance-based analysis of stability and transient performance is very effective. This can be traced back to the input-filter design rules for regulated converters proposed by Middlebrook in 1976 [29]. A cascaded system with a voltage-controlled source is stable if 1) the ratio of the source output impedance Z_{oS} to the load input impedance Z_{iL} satisfies the Nyquist stability criterion and 2) the source and load converters are stable individually, which means Z_{oS} (or $\frac{1}{Z_{oS}}$) and $\frac{1}{Z_{iL}}$ (or Z_{iL}) should be stable too. Subsequently, various impedance criteria aiming at more accurate and practical assessment of stability have been developed during the past four decades [30]–[33]. In [34], it is pointed out that, for cascaded systems with a current-controlled source, its stability is determined by the impedance ratio of Z_{iL} to Z_{oS} if the source output admittance $\frac{1}{Z_{oS}}$ is stable [34]. Moreover, the above impedance-based stability criteria have also been extended to three-phase AC cascaded systems [15], [35]–[37].

While these criteria are useful, it is very confusing to have different stability criteria for different systems. Moreover, when two converters are connected together, cascaded (series) connection is just one type. They can be connected in parallel too. For example, there are often several high-speed trains at a station, which effectively means many PWM-controlled rectifiers are operated in parallel. Instability incidents, e.g. low-frequency oscillations, of electric railway

vehicles have happened worldwide [38], mainly due to the parallel operation of rectifiers. Inverters can be operated in parallel too, which is very common nowadays in renewable integration [1], [5], [39]. Therefore, developing a generic stability criteria is very important.

Following the preliminary results reported in [40], the stability of general power electronic systems consisting of two converters/sources is considered. The two converters/sources can be connected in series or in parallel. After modeling converters/sources with the well-known Thevenin theorem and the Norton theorem, the stability of an individual converter/source is investigated and a generic impedance-sum stability criterion is proposed for systems with two individually stable converters/sources. Such a system is stable if and only if the sum of the individual impedances does not encircle the origin clockwise or, equivalently, the impedance sum does not have any right-half-plane (RHP) zeros. This criterion is applicable to both DC and AC systems. It does not depend on the connection type either, avoiding the dilemma of choosing the inverter or the grid as the source when investigating the stability of grid-connected inverters [34].

A sum type criterion was reported in [41] but it was proposed for Z+Z cascaded systems only, and with a particular application to hybrid energy storage systems. Different from [41], this paper proposes a generic stability criterion that is applicable to any power electronic system consisting of two converters/sources. The two converters/sources can be connected in series (cascaded) or in parallel, as illustrated in the paper as V-V systems, V-I systems, I-V systems and I-I systems. The stability of all the cases is rigorously proven and numerically illustrated. Moreover, in [41], only Z+Z cascaded DC systems, which correspond to V-V DC systems in this paper, were studied. The proposed generic stability criterion can be applied to both DC systems and AC systems, for example, grid-tied inverters, cascaded DC/DC systems, and inverters operated in parallel. Hence, the contribution of the paper with comparison to [41] is clear and significant. Furthermore, [41] states that the sum type criterion does not need the information about the RHP zeros of the impedance of individual converters. However, it is shown in this paper that it does affect the stability of the voltage or current source and, hence, the stability of the whole system, although this information does not explicitly appear in the impedance sum. In other words, it requires each individual converters/sources to be stable, which is practically true and hence reasonable.

The rest of this paper is organized as follows. In Section II, power electronic systems with two converters/sources are modeled after modeling and clarifying the stability of a single converter/source. Then, the generic stability criterion for power electronic systems with two individually stable converters/sources is proposed and proved theoretically in Section III. After that, the proposed stability criterion is applied to four typical systems and verified by results from OPAL RT OP4500 in Section IV. Finally, discussions and conclusions are made in Section V.

II. MODELING OF POWER ELECTRONIC SYSTEMS WITH TWO CONVERTERS/SOURCES

A. MODELING AND STABILITY OF A SINGLE CONVERTER/SOURCE

It is well known that the switching effect in power electronic converters can be ignored and linearized according to the averaging theory [42]–[44]. By doing this, as shown in Fig. 1, any power converter or source can be represented as a voltage source v in series with an impedance Z according to the Thevenin theorem, or as a current source i in parallel with the same impedance Z according to the Norton theorem. Some examples will be given in Section IV. The Norton and Thevenin models are equivalent and satisfy $v = i \cdot Z$. In practice, it is required that v and i are bounded in order to guarantee the stability of the converter/source.

For the Thevenin model shown in Fig. 1(b), the bus voltage and current are

$$v_{bus} = v - Z \cdot i_{bus}, \qquad i_{bus} = \frac{1}{Z}(v - v_{bus}).$$

Hence, in order for the converter/source having a bounded voltage source v to be stable, i.e., to have bounded v_{bus} and i_{bus} for any bounded i_{bus} and v_{bus}, respectively, both the impedance Z and its inverse $\frac{1}{Z}$ are required to be stable. The first condition is easy to understand. The second condition can be seen from the case when $v_{bus} = 0$, i.e., when the port is short-circuited. In this case, $i_{bus} = \frac{1}{Z}v$, which requires $\frac{1}{Z}$ to be stable in order for i_{bus} to be bounded for a bounded v. This is called short-circuit stable and it is well documented in classic circuit theory; see e.g., [45]. For the Norton model shown in Fig. 1(c), the bus voltage and current are

$$v_{bus} = Z(i - i_{bus}), \qquad i_{bus} = i - \frac{1}{Z}v_{bus}.$$

In order for i_{bus} to be bounded for a bounded i and a bounded v_{bus}, $\frac{1}{Z}$ is required to be stable according to the above equation on the right. Moreover, in order for the port voltage v_{bus} to be bounded when $i_{bus} = 0$, i.e. when it is open-circuited, Z is required to be stable according to the above equation on the left. This is called open-circuit stable and it is well documented in classic circuit theory; see e.g., [45] again. Hence, in order for a converter/source having a bounded current source i to be stable, both the impedance Z and its inverse are required to be stable. In other words, in order to guarantee the stability of the equivalent Thevenin and Norton models or the stability of a converter/source represented as a black-box, it implicitly requires that the voltage source v and the current source i are bounded and that both the impedance Z and its inverse $\frac{1}{Z}$ are stable. The fact that the impedance Z needs to be stable is well known but the fact that its inverse $\frac{1}{Z}$ needs to be stable at the same time is often neglected. Hence, this fact itself offers insights for the design of individual converters/sources: both the impedance Z and its inverse $\frac{1}{Z}$ should be stable. Otherwise, instability may occur. For example, the condition for $\frac{1}{Z}$ to be stable guarantees that the current of a voltage-controlled converter is bounded if there is a grid fault, such as short circuit. Similarly, the condition for Z

TABLE 1. All possible cases of systems with two converters/sources.

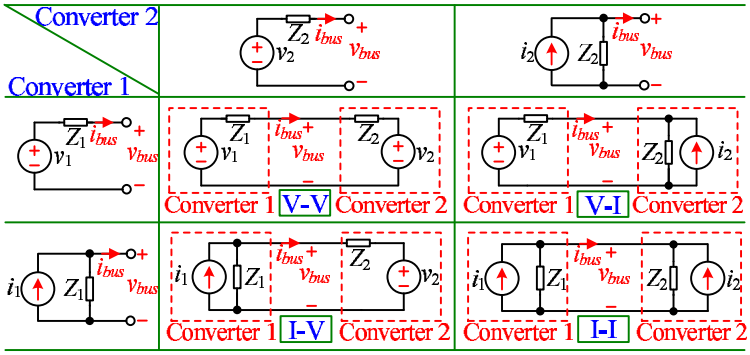

to be stable guarantees that the voltage remains bounded even if the grid is open-circuited for a grid-tied current-controlled converter. These are critical properties for converters, which are unfortunately neglected in many literature. In this paper, it is assumed that individual converters/sources are stable.

Normally, the Thevenin equivalent model is preferred when the impedance is small and the Norton equivalent model is preferred when the impedance is large. However, it does not really matter whether to use the Thevenin model or the Norton model because they are equivalent (under the conditions discussed above).

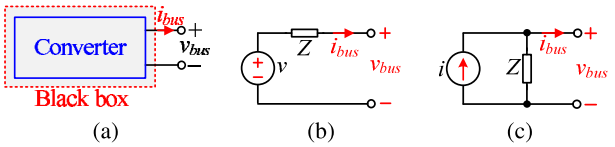

FIGURE 1. Modeling of a power converter/source: (a) as a black box; (b) as a Thevenin model; (c) as a Norton model.

It is worth highlighting that the modeling shown in Fig. 1 is applicable to both AC and DC systems. Hence, the stability criterion to be developed is applicable to both AC and DC systems.

B. ALL POSSIBLE CASES OF POWER ELECTRONIC SYSTEMS WITH TWO CONVERTERS/SOURCES

Since a power converter/source can be modeled as a non-ideal voltage or current source, when two power converter/sources are connected together, as shown in Table 1, there are four possible cases: a) to form a V-V system, i.e., a (non-ideal, omitted hereafter) voltage source connected with a voltage source, such as the parallel operation of voltage-controlled inverters; 2) to form an I-I system, i.e., a current source connected with a current source, such as the parallel operation of current-controlled converters; 3) to form an I-V system, i.e., a current source connected with a voltage source, such as a traditional current-controlled inverter connected to a weak grid; and 4) to form a V-I system, i.e., a voltage source connected with a current source, such as traditional cascaded DC/DC converters. Here, $Z_1(s)$ and $Z_2(s)$ are the impedances of the two converters/sources, respectively. These systems will be discussed in details in Section IV with illustrative examples. In the sequel, $Z_1(s)$ and $Z_2(s)$ are expressed as

$$Z_1(s) = N_1(s)/D_1(s) \tag{1}$$

$$Z_2(s) = N_2(s)/D_2(s) \tag{2}$$

to facilitate the presentation. They do not have to be rational. Note again that the impedances Z_1 and Z_2 may be large or small, depending on how the converter is controlled and how the converter is built [1].

III. GENERIC STABILITY CRITERION FOR POWER ELECTRONIC SYSTEMS WITH TWO CONVERTERS/SOURCES

Theorem 1: Regardless of the connection type, a power electronic system with two individually stable converters/sources is stable if and only if the sum of their impedances does not encircle the origin clockwise.

Proof: Since there are four different cases, as shown in Table 1, the proof is carried out below for V-V systems, I-I systems, I-V systems and V-I systems one by one.

(a) V-V Systems. As shown in the upper left corner of Table 1, its $i_{bus}(s)$ and $v_{bus}(s)$ can be expressed as

$$i_{bus}(s) = \frac{v_1 - v_2}{Z_1(s) + Z_2(s)} \tag{3}$$

$$v_{bus}(s) = v_2 + \frac{Z_2(s)\,(v_1 - v_2)}{Z_1(s) + Z_2(s)} \tag{4}$$

Substituting (1) and (2) into (3) and (4), $i_{bus}(s)$ and $v_{bus}(s)$ can be re-written as

$$i_{bus}(s) = \frac{D_1(s)D_2(s)\cdot(v_1 - v_2)}{N_1(s)D_2(s) + N_2(s)D_1(s)} \tag{5}$$

$$v_{bus}(s) = \frac{N_1(s)D_2(s)v_2 + N_2(s)D_1(s)v_1}{N_1(s)D_2(s) + N_2(s)D_1(s)} \tag{6}$$

The denominators of $i_{bus}(s)$ and $v_{bus}(s)$ are the same, i.e., $N_1(s)D_2(s) + N_2(s)D_1(s)$. Since the converters/sources are individually stable, v_1 and v_2 are bounded. Therefore, $N_1(s)D_2(s) + N_2(s)D_1(s) = 0$ is the characteristic equation of the system. In other words, the V-V system is stable if and

only if $N_1(s)D_2(s)+N_2(s)D_1(s)=0$ does not have any RHP roots.

By (1) and (2), Z_1+Z_2 can be expressed as

$$Z_1(s)+Z_2(s)=\frac{N_1(s)}{D_1(s)}+\frac{N_2(s)}{D_2(s)}=\frac{N_1(s)D_2(s)+N_2(s)D_1(s)}{D_1(s)D_2(s)}, \tag{7}$$

which means $N_1(s)D_2(s)+N_2(s)D_1(s)$ is also the numerator of Z_1+Z_2. Therefore, the roots of $N_1(s)D_2(s)+N_2(s)D_1(s)=0$ are the zeros of Z_1+Z_2. According to the well-known Cauchy's argument principle in complex analysis [46], Z_1+Z_2 does not have any RHP zeros, or equivalently the V-V system is stable, *if and only if* the number of times that the impedance sum Z_1+Z_2 encircles the origin clockwise is equal to the number of the unstable poles of Z_1+Z_2. Since the converters/sources are individually stable, Z_1 and Z_2 do not have any unstable poles. Hence, the V-V system with two individually stable converters/sources is stable *if and only if* the sum of impedances of individual converters/sources does not encircle the origin clockwise. This proves the theorem for V-V systems.

(b) I-I Systems. As shown in the lower right corner of Table 1, its $i_{bus}(s)$ and $v_{bus}(s)$ can be expressed as

$$i_{bus}(s)=i_1\frac{Z_1(s)}{Z_1(s)+Z_2(s)}-i_2\frac{Z_2(s)}{Z_1(s)+Z_2(s)} \tag{8}$$

$$v_{bus}(s)=(i_1+i_2)\frac{Z_1(s)Z_2(s)}{Z_1(s)+Z_2(s)} \tag{9}$$

Substituting (1) and (2) into (8) and (9), $i_{bus}(s)$ and $v_{bus}(s)$ can be rewritten as

$$i_{bus}(s)=\frac{N_1(s)D_2(s)i_1-N_2(s)D_1(s)i_2}{N_1(s)D_2(s)+N_2(s)D_1(s)} \tag{10}$$

$$v_{bus}(s)=\frac{N_1(s)N_2(s)\,(i_1+i_2)}{N_1(s)D_2(s)+N_2(s)D_1(s)} \tag{11}$$

Similar to V-V systems, the denominators of $i_{bus}(s)$ and $v_{bus}(s)$ in I-I systems are the same, i.e., $N_1(s)D_2(s)+N_2(s)D_1(s)$. Since the converters/sources are individually stable, i_1 and i_2 are bounded and Z_1 and Z_2 are stable, the I-I system is stable *if and only if* the sum of impedances of individual converters/sources does not encircle the origin clockwise. This proves the theorem for I-I systems.

(c) I-V Systems. As shown in the lower left corner of Table 1, its $i_{bus}(s)$ and $v_{bus}(s)$ can be expressed as

$$i_{bus}(s)=i_1\frac{Z_1(s)}{Z_1(s)+Z_2(s)}-v_2\frac{1}{Z_1(s)+Z_2(s)} \tag{12}$$

$$v_{bus}(s)=v_2\frac{Z_1(s)}{Z_1(s)+Z_2(s)}-i_1\frac{Z_1(s)Z_2(s)}{Z_1(s)+Z_2(s)} \tag{13}$$

Substituting (1) and (2) into (12) and (13), $i_{bus}(s)$ and $v_{bus}(s)$ can be rewritten as

$$i_{bus}(s)=\frac{N_1(s)D_2(s)i_1-D_1(s)D_2(s)v_2}{N_1(s)D_2(s)+N_2(s)D_1(s)} \tag{14}$$

$$v_{bus}(s)=\frac{N_1(s)D_2(s)v_2-N_1(s)N_2(s)i_1}{N_1(s)D_2(s)+N_2(s)D_1(s)} \tag{15}$$

Similar to the V-V and I-I systems, the denominators of $i_{bus}(s)$ and $v_{bus}(s)$ in the I-V system are the same, i.e., $N_1(s)D_2(s)+N_2(s)D_1(s)$. Since the converters/sources are individually stable, i_1 and v_2 are bounded and Z_1 and Z_2 are stable, the system is stable *if and only if* the sum of impedances of individual converters/sources does not encircle the origin clockwise.

(d) V-I Systems. As shown in the upper right corner of Table 1, its $i_{bus}(s)$ and $v_{bus}(s)$ can be expressed as

$$i_{bus}(s)=v_1\frac{1}{Z_1(s)+Z_2(s)}-i_2\frac{Z_2(s)}{Z_1(s)+Z_2(s)} \tag{16}$$

$$v_{bus}(s)=v_1\frac{Z_2(s)}{Z_1(s)+Z_2(s)}+i_2\frac{Z_1(s)Z_2(s)}{Z_1(s)+Z_2(s)} \tag{17}$$

Substituting (1) and (2) into (12) and (13), $i_{bus}(s)$ and $v_{bus}(s)$ can be rewritten as

$$i_{bus}(s)=\frac{D_1(s)D_2(s)v_1-N_2(s)D_1(s)i_2}{N_1(s)D_2(s)+N_2(s)D_1(s)} \tag{18}$$

$$v_{bus}(s)=\frac{N_2(s)D_1(s)v_1+N_1(s)N_2(s)i_2}{N_1(s)D_2(s)+N_2(s)D_1(s)} \tag{19}$$

Similar to the previous three cases, the denominators of $i_{bus}(s)$ and $v_{bus}(s)$ in the V-I system are the same, i.e., $N_1(s)D_2(s)+N_2(s)D_1(s)$. Since the converters/sources are individually stable, v_1 and i_2 are bounded and Z_1 and Z_2 are stable, the system is stable *if and only if* the sum of impedances of individual converters/sources does not encircle the origin clockwise.

In summary, Theorem 1 has been proven for any power electronic systems with two individually stable converters/sources.

The proof of Theorem 1 also indicates the corollary below.

Corollary 2: Regardless of the connection type, a power electronic system with two individually stable converters/sources is stable if and only if the impedance sum does not have any RHP zeros.

As a result, the system stability can be assessed by directly checking the number of RHP zeros of Z_1+Z_2, without drawing the Nyquist plot. Moreover, the proposed impedance-sum criterion does not need to know the connection type of the power converters/sources. For existing impedance-ratio criteria, it is necessary to know the connection type in order to select the correct impedance ratio: for an I-V system, the correct impedance ratio is $\frac{Z_2}{Z_1}$ and for a V-I system, the correct impedance ratio is $\frac{Z_1}{Z_2}$. However, for the proposed impedance-sum criterion, the impedance sum is always Z_1+Z_2, regardless of the connection type. Furthermore, it can be applied to DC systems and AC systems as well, which makes it very generic.

IV. APPLICATIONS

A. PARALLEL OPERATION OF VOLTAGE-CONTROLLED INVERTERS (V-V SYSTEMS)

Fig. 2 illustrates a system with two parallel-operated voltage-controlled inverters. This is a typical V-V system. In order to simplify the presentation, the two inverters are assumed to operate without a load.

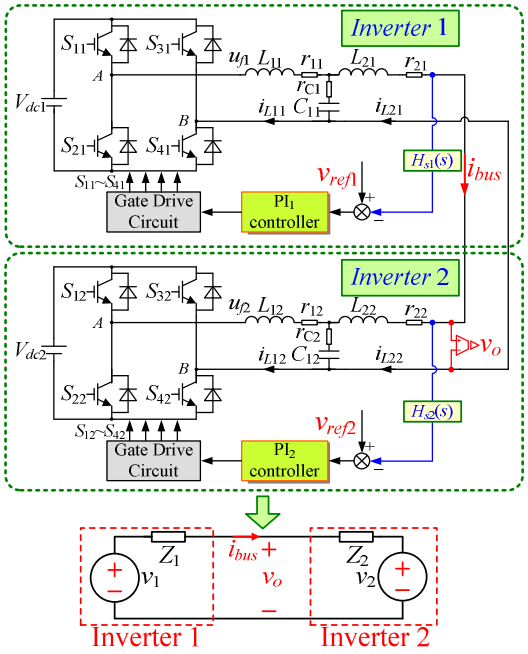

FIGURE 2. An example V-V system: voltage-controlled inverters in parallel operation without a load.

Before analyzing the stability of the V-V system, the impedance models of the individual inverters are firstly derived.

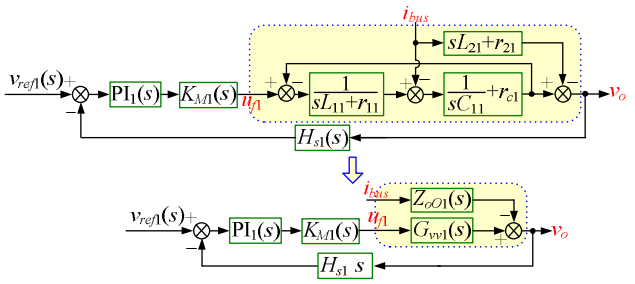

FIGURE 3. Block diagram of Inverter 1 in the example V-V system.

For Inverter 1 shown in Fig. 2, the simplified block diagram is depicted in Fig. 3, where the *LCL* filter part is represented by the transfer function $G_{vv1}(s)$ from the filter input voltage to the filter output voltage and the transfer function $Z_{oO1}(s)$ from the bus current i_{bus} to the filter output voltage described as

$$G_{vv1}(s) = \frac{1/sC_{11} + r_{C1}}{sL_{11} + r_{11} + 1/sC_{11} + r_{C1}} \tag{20}$$

$$Z_{oO1}(s) = \frac{(sL_{11} + r_{11}) \cdot (1/sC_{11} + r_{C1})}{(sL_{11} + r_{11}) + (1/sC_{11} + r_{c1})} + \frac{(sL_{11} + r_{11}) \cdot (sL_{21} + r_{21})}{(sL_{11} + r_{11}) + (1/sC_{11} + r_{c1})} + \frac{(sL_{21} + r_{21}) \cdot (1/sC_{11} + r_{C1})}{(sL_{11} + r_{11}) + (1/sC_{11} + r_{c1})} \tag{21}$$

According to Fig. 3, the output voltage v_o of Inverter 1 can be further derived as

$$v_o(s) = v_1(s) - Z_1(s) \cdot i_{bus}(s) \tag{22}$$

with

$$v_1(s) = \frac{T_{i1}(s)}{1 + T_{i1}(s)} \cdot \frac{v_{ref1}(s)}{H_{s1}(s)} \tag{23}$$

$$Z_1(s) = Z_{oO1}(s)/\left(1 + T_{i1}(s)\right) \tag{24}$$

$$T_{i1}(s) = PI_1(s)K_{M1}(s)G_{vv1}(s)H_{s1}(s). \tag{25}$$

Here, $PI_1(s) = K_{p1} + K_{i1}/s$ is the voltage controller and H_{s1} is the sampling coefficient of the output voltage. From the control point of view, the PWM conversion and the switching process can be ignored because the switching frequency is much higher than the line frequency. As a result, the inverter can be modeled by its gain $K_{M1}(s) = V_{dc1}/V_{tri1}$ [47], where V_{tri1} is the modulation carrier.

According to (22), the model of Inverter 1 can be depicted as shown in Fig. 2, which is composed of a voltage source $v_1(s)$ and a series-connected output impedance $Z_1(s)$.

Similarly, the model of Inverter 2 can also be derived and depicted as shown in Fig. 2, which is composed of a voltage source $v_2(s)$ and a series-connected output impedance $Z_2(s)$ with

$$v_2(s) = \frac{T_{i2}(s)}{1 + T_{i2}(s)} \cdot \frac{v_{ref2}(s)}{H_{s2}(s)} \tag{26}$$

$$Z_2(s) = \frac{Z_{oO2}(s)}{1 + T_{i2}(s)} \tag{27}$$

where $T_{i2}(s)$, $v_{ref2}(s)$, $H_{s2}(s)$ and $Z_{oO2}(s)$ have the same meanings as $T_{i1}(s)$, $v_{ref1}(s)$, $H_{s1}(s)$ and $Z_{oO1}(s)$, with the subscript 1 for Inverter 1 and the subscript 2 for Inverter 2.

TABLE 2. Parameters of two systems in Figure 2.

System A: Unstable V-V system

Parameter	*Value*	*Parameter*	*Value*	*Parameter*	*Value*
V_{dc1}, V_{dc2}	180 V	r_{11}	0.5 Ω	L_{22}	10 μH
f_{s1}, f_{s2}	10 kHz	L_{21}	4 μH	r_{22}	0.001 Ω
P_o	0 W	r_{21}	0.001 Ω	C_{12}, r_{C2}	10 μF, 0.2 Ω
v_{ref}	110 VAC	C_{11}, r_{C1}	5 μF, 0.1 Ω	PI_1	K_p=3, K_i=10
K_{M1}, K_{M2}	180	L_{12}	4 mH	PI_2	K_p=10, K_i=10
L_{11}	0.4 mH	r_{12}	1 Ω	H_{s1}, H_{s2}	1

System B: Stable V-V system

Parameter	*Value*	*Parameter*	*Value*	*Parameter*	*Value*
V_{dc1}, V_{dc2}	180 V	r_{11}	1 Ω	L_{22}	1.3 μH
f_{s1}, f_{s2}	10 kHz	L_{21}	1.3 μH	r_{22}	1 Ω
P_o	0 W	r_{21}	1 Ω	C_{12}, r_{C2}	50 μF, 0.1 Ω
v_{ref}	110 VAC	C_{11}, r_{C1}	50μF, 0.1Ω	PI_1	K_p=3, K_i=10
K_{M1}, K_{M2}	180	L_{12}	4 mH	PI_2	K_p=3, K_i=10
L_{11}	4 mH	r_{12}	1 Ω	H_{s1}, H_{s2}	1

In Table 3, two sets of parameters are given, with the Nyquist plots and the pole-zero map of the corresponding impedance sum $Z_1 + Z_2$ depicted in Fig. 4 and Fig. 5, respectively. Note that the Nyquist plots in this paper are only shown for the frequencies from $\omega = 0$ to $+\infty$. The other half corresponding to the frequency from $\omega = -\infty$ to 0, which

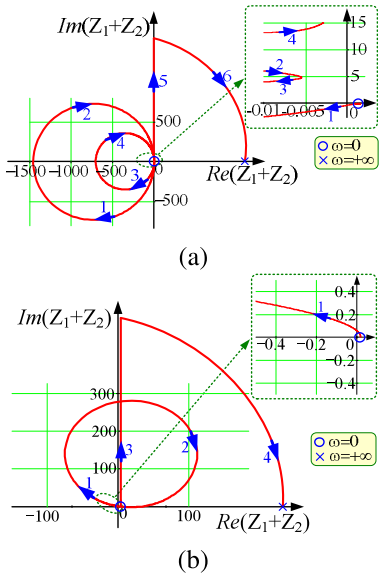

FIGURE 4. Nyquist plots of the impedance sum of the V-V systems in Table 3: (a) System A (Unstable); (b) System B (Stable).

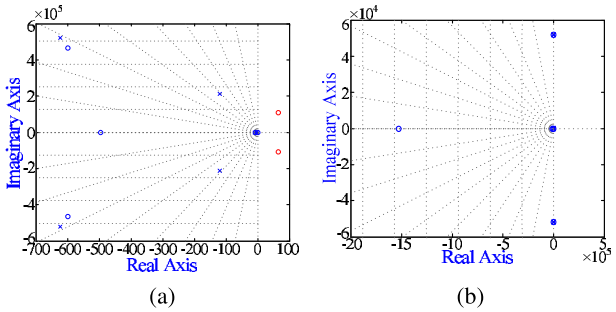

FIGURE 5. Pole-zero maps of the V-V systems in Table 3: (a) System A (Unstable); (b) System B (Stable).

is symmetric to the half shown, is omitted. Hence, the actual number of encirclements around the origin or $(-1, j0)$ should be doubled from the number obtained from the figure. As can be seen, for System A, the number of times the impedance sum $Z_1 + Z_2$ encircles the origin clockwise is $2 \times 1 = 2$, while for System B the number of times the impedance sum $Z_1 + Z_2$ encircles the origin clockwise is 0. Fig. 5 shows that the impedance sum $Z_1 + Z_2$ of System A has two RHP zeros but the impedance sum $Z_1 + Z_2$ of System B does not have any RHP zeros, which is consistent with the Nyquist plots. According to the impedance-sum criterion, System A is unstable but System B is stable.

As shown in (23) and (26), the voltage sources $v_1(s)$ and $v_2(s)$ in Fig. 2 depend on the loop gain of the individual inverter, respectively, which are bounded if the individual inverters are stable. As mentioned above, the stability of each individual inverter should be checked at first before using the proposed impedance-sum criterion to check the stability of the V-V system.

The above two V-V systems are built and tested with OPAL RT OP4500 and the results are shown in Fig. 6. System A is indeed unstable, as shown in Fig. 6(a), while System B is indeed stable, as shown in Fig. 6(b).

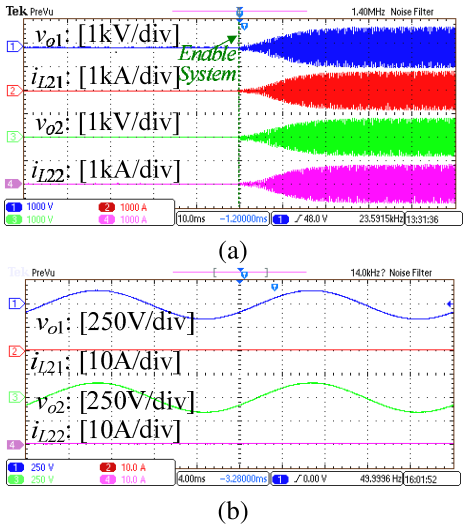

FIGURE 6. Test results of the V-V systems in Table 3: (a) System A (Unstable); (b) System B (Stable).

B. PARALLEL OPERATION OF CURRENT-CONTROLLED CONVERTERS (I-I SYSTEMS)

Fig. 7 illustrates a system with two parallel-operated current-controlled inverters. This is a typical I-I system. The two inverters operate in parallel with a resistive load.

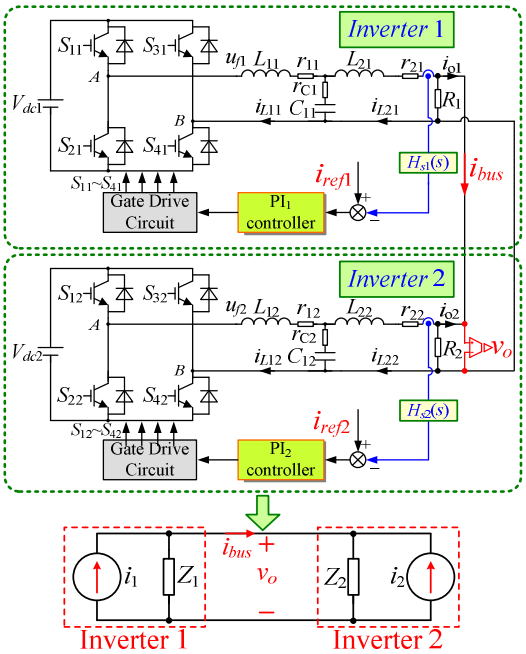

FIGURE 7. An example I-I system: Parallel-operated current-controlled inverters with a resistive load.

Before analyzing the stability of the I-I system, the models of the individual inverters are firstly derived.

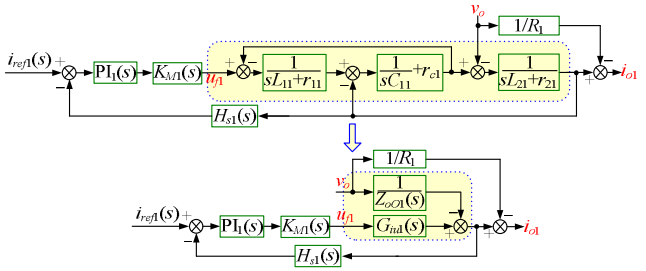

FIGURE 8. Simplified block diagram of Inverter 1 in the example I-I system.

For Inverter 1 shown in Fig. 7, the simplified block diagram is depicted in Fig. 8, where the *LCL* filter part is represented by the transfer function $Z_{oO1}(s)$ from the filter output current to the output voltage and the transfer function $G_{iu1}(s)$ from the filter input voltage to the filter output current. $Z_{oO1}(s)$ is the same as the one shown in (21) and $G_{iu1}(s)$ can be found via

$$\begin{aligned}\frac{1}{G_{iu1}(s)} = &\frac{(sL_{11}+r_{11})\cdot(1/sC_{11}+r_{C1})}{1/sC_{11}+r_{C1}} \\ &+\frac{(sL_{11}+r_{11})\cdot(sL_{21}+r_{21})}{1/sC_{11}+r_{C1}} \\ &+\frac{(sL_{21}+r_{21})\cdot(1/sC_{11}+r_{C1})}{1/sC_{11}+r_{C1}}\end{aligned} \tag{28}$$

According to Fig. 8, the output current i_{o1} of Inverter 1 can be further derived as

$$i_{o1}(s) = i_1(s) - \frac{1}{Z_1(s)}\cdot v_o(s) \tag{29}$$

with

$$i_1(s) = \frac{T_{i1}(s)}{1+T_{i1}(s)}\cdot\frac{i_{ref1}(s)}{H_{s1}(s)} \tag{30}$$

$$Z_1(s) = \frac{Z_{oO1}(s)\cdot(1+T_{i1}(s))\cdot R_1}{Z_{oO1}(s)\cdot(1+T_{i1}(s))+R_1} \tag{31}$$

$$T_{i1}(s) = PI_1(s)K_{M1}(s)G_{iu1}(s)H_{s1}(s). \tag{32}$$

Here, $PI_1(s) = K_{p1} + K_{i1}/s$ is the current controller of Inverter 1, H_{s1} is the sampling coefficient of the output current and R_1 is the resistive load. $K_{M1}(s) = V_{dc1}/V_{tri1}$ is the gain of the inverter [47], where V_{tri1} is the modulation carrier of Inverter 1.

According to (29), the model of Inverter 1 can be depicted as shown in Fig. 7, which is composed of a current source $i_1(s)$ and a parallel-connected output impedance $Z_1(s)$.

Similarly, the model of Inverter 2 can also be depicted as shown in Fig. 7, which is composed of a current source $i_2(s)$ and a parallel-connected output impedance $Z_2(s)$ given by

$$i_2(s) = \frac{T_{i2}(s)}{1+T_{i2}(s)}\cdot\frac{i_{ref2}(s)}{H_{s2}(s)} \tag{33}$$

$$Z_2(s) = \frac{Z_{oO2}(s)\cdot(1+T_{i2}(s))\cdot R_2}{Z_{oO2}(s)\cdot(1+T_{i2}(s))+R_2}. \tag{34}$$

Here, $T_{i2}(s)$, $i_{ref2}(s)$, $H_{s2}(s)$, R_2 and $Z_{oO2}(s)$ have the same meanings as $T_{i1}(s)$, $i_{ref1}(s)$, $H_{s1}(s)$, R_1 and $Z_{oO1}(s)$, with the subscript 2 representing Inverter 2.

TABLE 3. Parameters of two systems in Figure 7.

System A: Unstable I-I system

Parameter	Value	Parameter	Value	Parameter	Value
V_{dc1}, V_{dc2}	180 V	r_{11}	0.05 Ω	L_{22}	1.3 μH
f_{s1}, f_{s2}	10 kHz	L_{21}	4 μH	r_{22}	0.001 Ω
R_1, R_2	10 Ω	r_{21}	0.001 Ω	C_{12}, r_{C2}	100μF, 0.01 Ω
i_{ref}	10 A AC	C_{11}, r_{C1}	2 μF, 0.1 Ω	PI_1	K_p=3,K_i=100
K_{M1} , K_{M2}	180	L_{12}	4 mH	PI_2	K_p=100,K_i=1
L_{11}	0.1 mH	r_{12}	0.01 Ω	H_{s1}, H_{s2}	1

System B: Stable I-I system

Parameter	Value	Parameter	Value	Parameter	Value
V_{dc1}, V_{dc2}	180 V	r_{11}	0.1 Ω	L_{22}	3.9 μH
f_{s1}, f_{s2}	10 kHz	L_{21}	3.9 μH	r_{22}	0.1 Ω
R_1, R_2	10 Ω	r_{21}	0.1 Ω	C_{12}, r_{C2}	10μF, 0.1 Ω
i_{ref}	10 A AC	C_{11}, r_{C1}	10μF, 0.1Ω	PI_1	K_p=10,K_i=100
K_{M1} , K_{M2}	180	L_{12}	4 mH	PI_2	K_p=10,K_i=100
L_{11}	4 mH	r_{12}	0.1 Ω	H_{s1}, H_{s2}	1

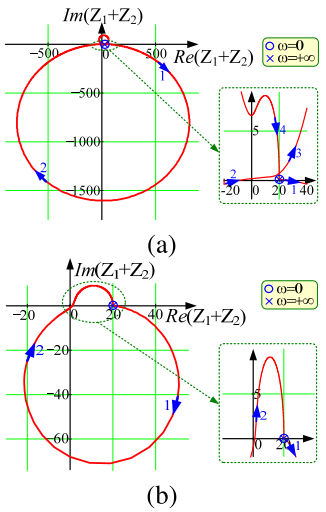

FIGURE 9. Nyquist plots of the impedance sum of the I-I systems in Table 2: (a) System A (Unstable); (b) System B (Stable).

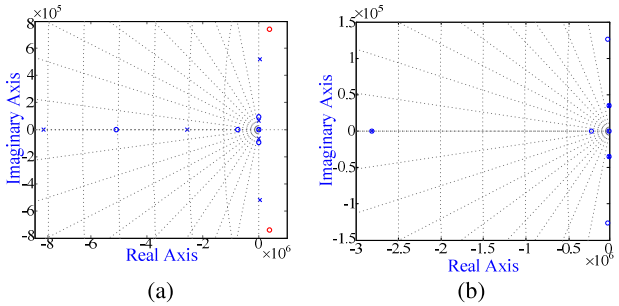

FIGURE 10. Pole-zero maps of the I-I systems in Table 2: (a) System A (Unstable); (b) System B (Stable).

In Table 2, two sets of parameters are given, with the Nyquist plots and the pole-zero map of the impedance sum Z_1+Z_2 depicted in Fig. 9 and Fig. 10, respectively. As can be seen, for System A, the number of times the impedance sum Z_1+Z_2 encircles the origin clockwise is $2\times 1 = 2$, while, for System B, the number of times the impedance sum $Z_1 + Z_2$

encircles the origin clockwise is 0. Fig. 10 shows that the impedance sum $Z_1 + Z_2$ of System A has two RHP zeros but $Z_1 + Z_2$ of System B does not have any RHP zeros. Therefore, according to the proposed impedance-sum criterion, System A is unstable but System B is stable.

Similar to the V-V system, the current sources $i_1(s)$ and $i_2(s)$ in Fig. 7 depend on the loop gain of the individual inverter, respectively, which are bounded if the individual inverters are stable. As mentioned above, the stability of each individual inverter should be checked at first before using the impedance-sum criterion to check the stability of the system.

The above two I-I systems are built and tested with OPAL RT OP4500 and the results are shown in Fig. 11. System A is indeed unstable, as shown in Fig. 11(a), and System B is indeed stable, as shown in Fig. 11(b).

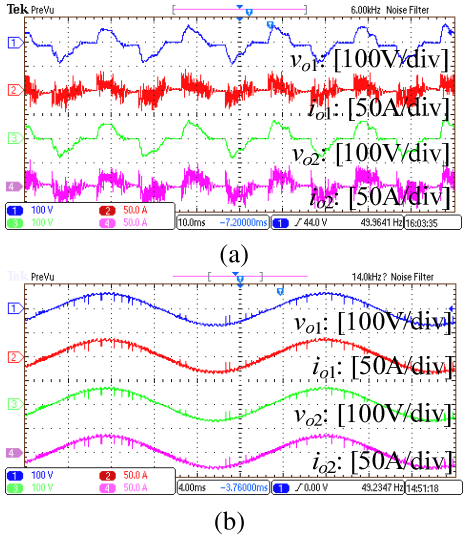

FIGURE 11. Test results of the I-I systems in Table 2: (a) System A (Unstable); (b) System B (Stable).

C. GRID-CONNECTED CURRENT-CONTROLLED INVERTERS (I-V SYSTEMS)

Fig. 12 illustrates a current-controlled inverter connected to a weak grid. This is a typical I-V system.

Since the inverter in the I-V system is the same as the inverter in the I-I system, it also has the same model as the inverter in the I-I system in Section IV-B, which is composed of a current source $i(s)$ and a parallel-connected output impedance $Z_1(s)$. Here, $i(s)$ and $Z_1(s)$ can be derived from (30) and (31) with $R_1 = \infty$ as

$$i(s) = \frac{T_i(s)}{1 + T_i(s)} \cdot \frac{i_{ref}(s)}{H_s(s)} \tag{35}$$

$$Z_1(s) = Z_{oO}(s) \cdot (1 + T_i(s)) . \tag{36}$$

Here, $T_i(s)$, $i_{ref}(s)$, $H_s(s)$ and $Z_{oO}(s)$ have the same meanings as $T_{i1}(s)$, $i_{ref1}(s)$, $H_{s1}(s)$ and $Z_{oO1}(s)$ in Section IV-B, respectively.

According to Fig. 12, the weak grid can be modeled as a non-ideal voltage source, which is composed of an ideal gird

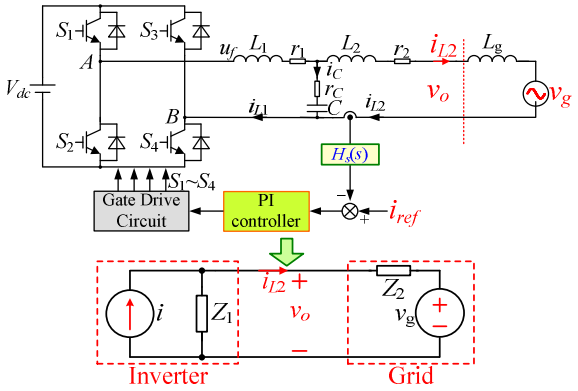

FIGURE 12. An example I-V system: a current-controlled inverter connected to a weak grid.

voltage $v_g(s)$ and a series-connected impedance $Z_2(s)$. Here, $Z_2(s)$ can be expressed as

$$Z_2(s) = sL_g \tag{37}$$

TABLE 4. Parameters of two systems in Figure 12.

Inverter				*Weak grid*	
Para.	*Value*	*Para.*	*Value*	System A: Unstable system	
V_{dc}	405 V	L_1	7.2 mH	v_g	220V/50Hz
f_s	8 kHz	R_1	0.01 Ω	L_g	2.5 mH
P_o	1.4 kW	L_2	1.2 mH	System B: Stable system	
H_s	0.55	R_2	0.01 Ω	v_g	220V/50Hz
K_{p1}	35	C	6 μH	L_g	0.1 mH
K_{i1}	60000	r_C	10 Ω	*Only L_g changed*	

In Table 4, two sets of I-V parameters are given. Here, only the grid inductance is different while the other parameters are the same in order to clearly show the impact of the grid inductance on the system stability. The Nyquist plots and the pole-zero map of the impedance sum $Z_1 + Z_2$ are depicted in Fig. 13 and Fig. 14, respectively. For System A, the number of times $Z_1 + Z_2$ encircles the origin clockwise is $2 \times 1 = 2$, while, for System B, the number of times $Z_1 + Z_2$ encircles the origin clockwise is 0. Fig. 14 shows that $Z_1 + Z_2$ of System

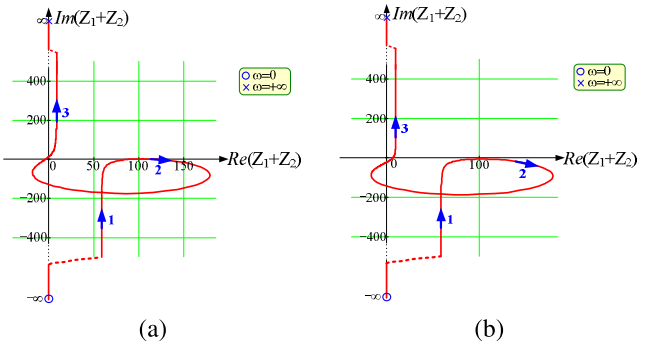

FIGURE 13. Nyquist plots of the impedance sum of the I-V systems in Table 4: (a) System A (Unstable); (b) System B (Stable).

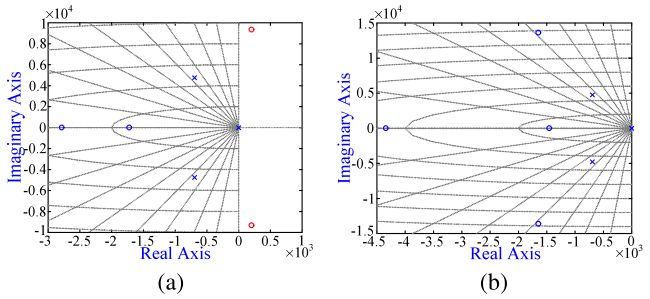

FIGURE 14. Pole-zero maps of the I-V systems in Table 4: (a) System A (Unstable); (b) System B (Stable).

A has two RHP zeros but $Z_1 + Z_2$ of System B does not have any RHP zeros. Therefore, according to the proposed impedance-sum criterion, System A is unstable but System B is stable.

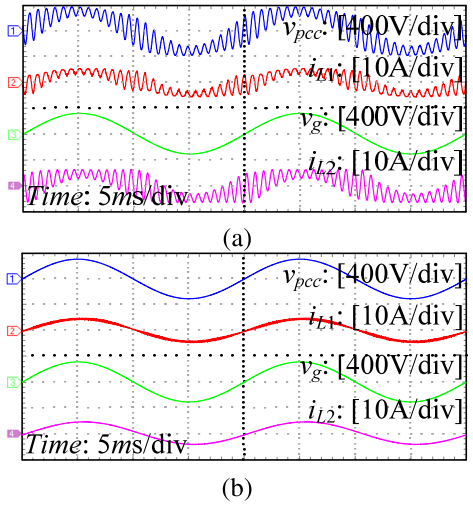

FIGURE 15. Test results of the I-V systems in Table 4: (a) System A (Unstable); (b) System B (Stable).

The above two I-V systems are built and tested with OPAL RT OP4500 and the results are shown in Fig. 15. System A is indeed unstable, as shown in Fig. 15(a), and System B is indeed stable, as shown in Fig. 15(b).

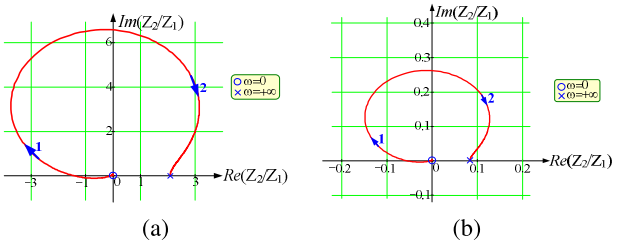

FIGURE 16. Nyquist plots of the impedance ratio $\frac{Z_2}{Z_1}$ of the I-V systems in Table 4: (a) System A (Unstable); (b) System B (Stable).

The stability of this kind of systems has been widely studied with impedance-ratio criteria, e.g. the one shown in [34]. According to the Nyquist plots of the impedance ratio $\frac{Z_2}{Z_1}$ of the systems shown in Fig. 16, it can be seen that System A is unstable while System B is stable after checking the encirclements around $(-1, j0)$. This is consistent with the conclusion from the proposed impedance-sum criterion.

Here, the purpose is to illustrate the proposed impedance-sum criterion so the impact of phase-locked-loop (PLL) [21], [48] and the delay caused by digital control [49], [50] are not considered. If considered, the expressions of $i(s)$ and $Z_1(s)$ in the model of the grid-connected inverter would change. But the same impedance-sum criterion can still be applied.

D. CASCADED DC/DC CONVERTERS (V-I SYSTEMS)

Fig. 17 illustrates a widely-used system with cascaded DC/DC converters. This is a typical V-I system, which consists of two voltage-controlled Buck converters. The upstream converter is often called the source converter and the downstream converter is called the load converter. The source converter, Converter 1, can be modeled as an ideal voltage source v_1 in series with its impedance $Z_1(s)$. The load converter, Converter 2, can be modeled as an ideal current source i_2 in parallel with its impedance $Z_2(s)$, where i_2 in this case is often negative. Since the models of converters in cascaded DC/DC converters have already been extensively studied, e.g. in [51] and [52], the models from the literature are directly adopted.

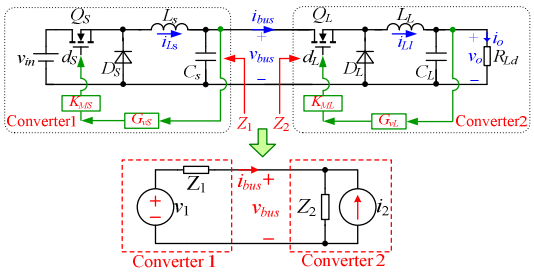

FIGURE 17. An example V-I system: cascaded DC/DC converters.

According to the small-signal circuit model of the Buck converter [51], [52], $Z_1(s)$ can be expressed as

$$Z_1(s) = \frac{Z_{oOS}(s)}{1 + T_{vS}(s)} \tag{38}$$

where $Z_{oOS}(s)$ is its open-loop output impedance and $T_{vS}(s) = G_{vS}(s)K_{MS}G_{vdS}(s)$ is the gain of the voltage loop. Here, $G_{vS}(s)$ and K_{MS} are the voltage controller and the gain of the converter, respectively. $G_{vdS}(s)$ is the transfer function from the duty cycle to the output voltage. The expressions of $G_{vdS}(s)$ and $Z_{oOS}(s)$ can be found in [51] and [52] and are omitted here.

According to [51] and [52], $Z_2(s)$ can be expressed as

$$Z_2(s) = \frac{(1 + T_{vL}(s))\, Z_{iOL}(s)G_{vdL}(s)}{G_{vdL}(s) - T_{vL}(s)(G_{vdL}(s) - Z_{iOL}(s)G_{idL}(s)G_{vOL}(s))} \tag{39}$$

where $Z_{ioL}(s)$ is its open-loop input impedance and $T_{vL}(s) = G_{vL}(s)K_{ML}G_{vdL}(s)$ is the gain of the voltage loop.

Here, $G_{vL}(s)$ and K_{ML} are the voltage controller and the gain of the converter, respectively. $G_{idL}(s)$, $G_{vOL}(s)$ and $G_{vdL}(s)$ are the transfer functions from the duty cycle to the input current, from the input voltage to the output voltage and from the duty cycle to the output voltage, respectively. The expressions of $Z_{ioL}(s)$, $G_{idL}(s)$, $G_{vOL}(s)$ and $G_{vdL}(s)$ can be found in [51] and [52] and are omitted here.

TABLE 5. Parameters of two systems in Figure 17.

System A: Unstable V-I system

v_{in}	48V	v_o	24V	f_{sS}	20kHz	L_S	1mH	L_L	450μH	K_{MS}	1/2.34
v_{bus}	32V	P_o	100W	f_{sL}	100kHz	C_S	150μF	C_L	220μF	K_{ML}	1/2.34

$$G_{vS}=5+\frac{100}{s} \qquad G_{vL}=3.723\cdot10^{9}\cdot\left(\frac{s+6.356\cdot10^{3}}{s+6.283\cdot10^{5}}\right)^{2}$$

System B: Stable V-I system

v_{in}	48V	v_o	24V	f_{sS}	20kHz	L_S	1mH	L_L	450μH	K_{MS}	1/2.34
v_{bus}	32V	P_o	100W	f_{sL}	100kHz	C_S	1.1mF	C_L	220μF	K_{ML}	1/2.34

$$G_{vS}=0.1+\frac{10}{s} \qquad G_{vL}=3.723\cdot10^{9}\cdot\left(\frac{s+6.356\cdot10^{3}}{s+6.283\cdot10^{5}}\right)^{2}$$

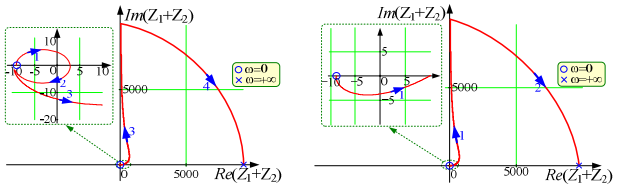

(a) (b)

FIGURE 18. Nyquist plots of the impedance sum of the V-I systems in Table 5: (a) System A (Unstable); (b) System B (Stable).

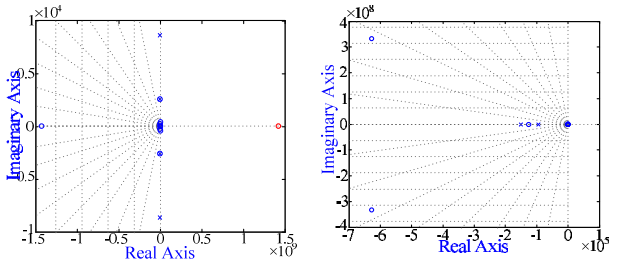

(a) (b)

FIGURE 19. Pole-zero maps of the V-I systems in Table 5: (a) System A (Unstable); (b) System B (Stable).

In Table 5, two sets of parameters are given, with the Nyquist plots and the pole-zero map of the corresponding impedance sum $Z_1 + Z_2$ depicted in Fig. 18 and Fig. 19, respectively. As can be seen, for System A, the number of times the impedance sum $Z_1 + Z_2$ encircles the origin clockwise is $2 \times 0.5 = 1$, while, for System B, the number of times the impedance sum Z_1+Z_2 encircles the origin clockwise is 0. Fig. 19 shows that the impedance sum Z_1+Z_2 of System A has one RHP zero but Z_1+Z_2 of System B does not have any RHP zeros. Therefore, according to the proposed impedance-sum criterion, System A is unstable but System B is stable.

The above two V-I systems are built and tested with OPAL RT OP4500 and the results are shown in Fig. 20. System A is indeed unstable, as shown in Fig. 20(a), and System B is indeed stable, as shown in Fig. 20(b).

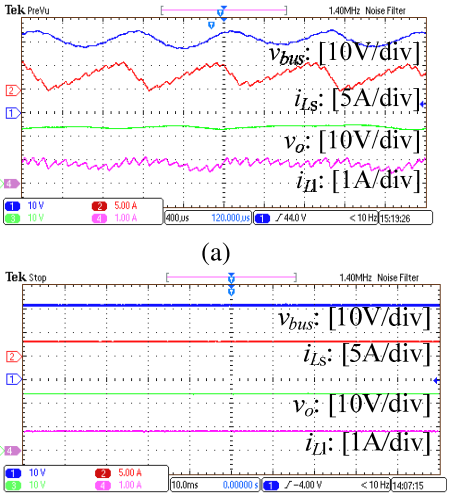

(a) (b)

FIGURE 20. Test results of the V-I systems in Table 5: (a) System A (Unstable); (b) System B (Stable).

This case has been widely studied with the well-known Middlebrook criterion [29]. For comparison, the Nyquist plots of the impedance ratio of $\frac{Z_1}{Z_2}$ of the systems are shown in Fig. 21. It can be seen that System A is unstable while System B is stable, which is consistent with the conclusion from the proposed impedance-sum criterion.

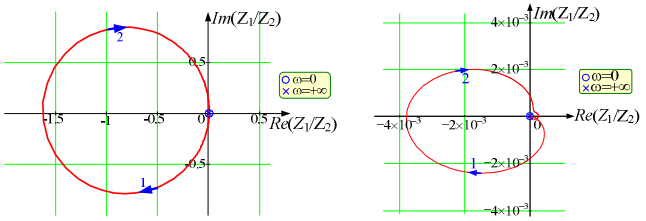

(a) (b)

FIGURE 21. Nyquist plots of the impedance ratio $\frac{Z_1(s)}{Z_2(s)}$ of the V-I systems in Table 5: (a) System A (Unstable); (b) System B (Stable).

According to the above applications, the proposed impedance-sum criterion has been proved effective to assess the stability of V-V systems, I-I systems, I-V systems and V-I stems as a general criterion regardless of the connection type of individually stable converters/sources.

V. DISCUSSIONS AND CONCLUSIONS

A generic impedance-sum stability criterion has been proposed for power electronic systems with two converters/sources. Different from traditional impedance-ratio criteria, the proposed criterion takes the form of the impedance sum. According to the proposed stability criterion, such a system with individually stable converters/sources is stable

if and only if the sum of the individual impedances does not encircle the origin clockwise or, equivalently, the impedance sum does not have any RHP zeros. The proposed criterion is applicable to all four possible cases of power electronic systems with two converters/sources connected in parallel or in series, including the V-V systems, the I-I systems, the I-V systems and the V-I systems. Moreover, the proposed stability criterion also provides a simple and clear approach to assess the system stability by directly checking whether the impedance sum has any RHP zeros or not. Thus, compared with existing impedance-ratio criteria, the impedance-sum criterion provides a convenient approach to evaluate system stability regardless of the connection types of its converters and is applicable to DC systems and AC systems. The test results from OPAL RT OP4500 of four different cases have demonstrated the effectiveness of the proposed criterion.

One insight obtained from this study is that the impedance of each individual converter/source should not have any RHP zeros or RHP poles. Moreover, the impedance sum should not have any RHP zeros either. Note that naturally the impedance sum does not have any RHP poles because each individual impedance does not have any.

Since current-controlled converters have high impedance magnitude than voltage-controlled converters, the stability of a system consisting of a current-controlled converter and a voltage-controlled converter/source is mainly affected by the current-controlled converter, according to the proposed impedance-sum criterion. For instance, in the example I-V system in Fig. 12, the current-controlled inverter is the main reason of system instability; in the example V-I system in Fig. 17, the load converter which is controlled as an constant power load is usually the main reason of system instability. These conclusions are consistent with practical phenomena and existing conclusions. How to apply this criterion in converter design to guarantee the stability of two converters/sources is being carried out. The extension of this work to power electronic systems with multiple converters/sources is also being investigated.

ACKNOWLEDGMENT

This paper was presented in part at the 20th IFAC World Congress, Toulouse, France, in 2017.

REFERENCES

[1] Q.-C. Zhong and T. Hornik, *Control of Power Inverters in Renewable Energy and Smart Grid Integration*. Hoboken, NJ, USA: Wiley, 2013.

[2] R. Turner, S. Walton, and R. Duke, "Stability and bandwidth implications of digitally controlled grid-connected parallel inverters," *IEEE Trans. Ind. Electron.*, vol. 57, no. 11, pp. 3685–3694, Nov. 2010.

[3] R. Haroun, A. Cid-Pastor, A. El Aroudi, and L. Martinez-Salamero, "Synthesis of canonical elements for power processing in DC distribution systems using cascaded converters and sliding-mode control," *IEEE Trans. Power Electron.*, vol. 29, no. 3, pp. 1366–1381, Mar. 2014.

[4] Q.-C. Zhong, "Synchronized and democratized smart grids to underpin the third industrial revolution," *IFAC-PapersOnLine*, vol. 50, no. 1, pp. 3592–3597, Jul. 2017.

[5] Q.-C. Zhong, "Power electronics-enabled autonomous power systems: Architecture and technical routes," *IEEE Trans. Ind. Electron.*, vol. 64, no. 7, pp. 5907–5918, Jul. 2017.

[6] S. Liu, P. X. Liu, and X. Wang, "Stability analysis of grid-interfacing inverter control in distribution systems with multiple photovoltaic-based distributed generators," *IEEE Trans. Ind. Electron.*, vol. 63, no. 12, pp. 7339–7348, Dec. 2016.

[7] S. Vesti, T. Suntio, J. A. Oliver, R. Prieto, and J. A. Cobos, "Impedance-based stability and transient-performance assessment applying maximum peak criteria," *IEEE Trans. Power Electron.*, vol. 28, no. 5, pp. 2099–2104, May 2013.

[8] W. Du, J. Zhang, Y. Zhang, and Z. Qian, "Stability criterion for cascaded system with constant power load," *IEEE Trans. Power Electron.*, vol. 28, no. 4, pp. 1843–1851, Apr. 2013.

[9] N. Mukherjee and D. Strickland, "Control of cascaded DC–DC converter-based hybrid battery energy storage systems—Part I: Stability issue," *IEEE Trans. Ind. Electron.*, vol. 63, no. 4, pp. 2340–2349, Apr. 2016.

[10] N. Bottrell, M. Prodanovic, and T. C. Green, "Dynamic stability of a microgrid with an active load," *IEEE Trans. Power Electron.*, vol. 28, no. 11, pp. 5107–5119, Nov. 2013.

[11] A. Emadi, A. Khaligh, C. H. Rivetta, and G. A. Williamson, "Constant power loads and negative impedance instability in automotive systems: Definition, modeling, stability, and control of power electronic converters and motor drives," *IEEE Trans. Veh. Technol.*, vol. 55, no. 4, pp. 1112–1125, Jul. 2006.

[12] X. Zhang, D. M. Vilathgamuwa, K. J. Tseng, B. S. Bhangu, and C. J. Gajanayake, "Power buffer with model predictive control for stability of vehicular power systems with constant power loads," *IEEE Trans. Power Electron.*, vol. 28, no. 12, pp. 5804–5812, Dec. 2013.

[13] D. Marx, P. Magne, B. Nahid-Mobarakeh, S. Pierfederici, and B. Davat, "Large signal stability analysis tools in dc power systems with constant power loads and variable power loads;a review," *IEEE Trans. Power Electron.*, vol. 27, no. 4, pp. 1773–1787, Apr. 2012.

[14] A. Khaligh, "Realization of parasitics in stability of DC–DC converters loaded by constant power loads in advanced multiconverter automotive systems," *IEEE Trans. Ind. Electron.*, vol. 55, no. 6, pp. 2295–2305, Jun. 2008.

[15] B. Wen, D. Boroyevich, R. Burgos, P. Mattavelli, and Z. Shen, "Small-signal stability analysis of three-phase AC systems in the presence of constant power loads based on measured d-q frame impedances," *IEEE Trans. Power Electron.*, vol. 30, no. 10, pp. 5952–5963, Oct. 2015.

[16] N. Jelani, M. Molinas, and S. Bolognani, "Reactive power ancillary service by constant power loads in distributed AC systems," *IEEE Trans. Power Del.*, vol. 28, no. 2, pp. 920–927, Apr. 2013.

[17] J. M. Espi and J. Castello, "Wind turbine generation system with optimized DC-link design and control," *IEEE Trans. Ind. Electron.*, vol. 60, no. 3, pp. 919–929, Mar. 2013.

[18] T. Messo, J. Jokipii, J. Puukko, and T. Suntio, "Determining the value of DC-link capacitance to ensure stable operation of a three-phase photovoltaic inverter," *IEEE Trans. Power Electron.*, vol. 29, no. 2, pp. 665–673, Feb. 2014.

[19] B. Wen, D. Boroyevich, P. Mattavelli, Z. Shen, and R. Burgos, "Influence of phase-locked loop on input admittance of three-phase voltage-source converters," in *Proc. 28th Annu. IEEE Appl. Power Electron. Conf. Expo. (APEC)*, Mar. 2013, pp. 897–904.

[20] D. Dong, B. Wen, D. Boroyevich, P. Mattavelli, and Y. Xue, "Analysis of phase-locked loop low-frequency stability in three-phase grid-connected power converters considering impedance interactions," *IEEE Trans. Ind. Electron.*, vol. 62, no. 1, pp. 310–321, Jan. 2015.

[21] C. Zhang, X. Wang, F. Blaabjerg, W. Wang, and C. Liu, "The influence of phase-locked loop on the stability of single-phase grid-connected inverter," in *Proc. IEEE Energy Convers. Congr. Expo. (ECCE)*, Sep. 2015, pp. 4737–4744.

[22] G. C. Konstantopoulos, Q.-C. Zhong, B. Ren, and M. Krstic, "Bounded droop controller for parallel operation of inverters," *Automatica*, vol. 53, pp. 320–328, Mar. 2015.

[23] G. C. Konstantopoulos, Q.-C. Zhong, B. Ren, and M. Krstic, "Stability analysis and fail-safe operation of inverters operated in parallel," *Int. J. Control*, vol. 88, no. 7, pp. 1410–1421, 2015.

[24] M. N. Marwali, J.-W. Jung, and A. Keyhani, "Stability analysis of load sharing control for distributed generation systems," *IEEE Trans. Energy Convers.*, vol. 22, no. 3, pp. 737–745, Sep. 2007.

[25] X. Wang, F. Blaabjerg, and W. Wu, "Modeling and analysis of harmonic stability in an AC power-electronics-based power system," *IEEE Trans. Power Electron.*, vol. 29, no. 12, pp. 6421–6432, Dec. 2014.

[26] F. Wang, J. L. Duarte, M. A. M. Hendrix, and P. F. Ribeiro, "Modeling and analysis of grid harmonic distortion impact of aggregated DG inverters," *IEEE Trans. Power Electron.*, vol. 26, no. 3, pp. 786–797, Mar. 2011.

[27] X. Wang, F. Blaabjerg, M. Liserre, Z. Chen, J. He, and Y. Li, "An active damper for stabilizing power-electronics-based AC systems," *IEEE Trans. Power Electron.*, vol. 29, no. 7, pp. 3318–3329, Jul. 2014.

[28] H. Bai, X. Wang, P. C. Loh, and F. Blaabjerg, "Passivity enhancement of grid-tied converters by series LC-filtered active damper," *IEEE Trans. Ind. Electron.*, vol. 64, no. 1, pp. 369–379, Jan. 2017.

[29] R. D. Middlebrook, "Input filter considerations in design and application of switching regulators," in *Proc. IEEE IAS*, May 1976, pp. 366–382.

[30] C. M. Wildrick, F. C. Lee, B. H. Cho, and B. Choi, "A method of defining the load impedance specification for a stable distributed power system," *IEEE Trans. Power Electron.*, vol. 10, no. 3, pp. 280–285, May 1995.

[31] P. Huynh and B. H. Cho, "A new methodology for the stability analysis of large-scale power electronics systems," *IEEE Trans. Circuits Syst. I, Fundam. Theory Appl.*, vol. 45, no. 4, pp. 377–385, Apr. 1998.

[32] H. H. C. Iu and C. K. Tse, "Study of low-frequency bifurcation phenomena of a parallel-connected boost converter system via simple averaged models," *IEEE Trans. Circuits Syst. I, Fundam. Theory Appl.*, vol. 50, no. 5, pp. 679–685, May 2003.

[33] X. Wang, R. Yao, and F. Rao, "Subsystem-interaction restraint in the two-stage DC distributed power systems with decoupling-controlled-integration structure," *IEEE Trans. Ind. Electron.*, vol. 52, no. 6, pp. 1555–1563, Dec. 2005.

[34] J. Sun, "Impedance-based stability criterion for grid-connected inverters," *IEEE Trans. Power Electron.*, vol. 26, no. 11, pp. 3075–3078, Nov. 2011.

[35] M. Belkhayat, "Stability criteria for ac power systems with regulated loads," Ph.D. dissertation, Dept. Elect. Comput. Eng., Purdue Univ. West Lafayette, IN, USA, Nov. 1997.

[36] W. Yao, M. Chen, J. Matas, J. M. Guerrero, and Z.-M. Qian, "Design and analysis of the droop control method for parallel inverters considering the impact of the complex impedance on the power sharing," *IEEE Trans. Ind. Electron.*, vol. 58, no. 2, pp. 576–588, Feb. 2011.

[37] A. Houari, H. Renaudineau, B. Nahid-Mobarakeh, J. P. Martin, S. Pierfederici, and F. Meibody-Tabar, "Large signal stability analysis and stabilization of converters connected to grid through *LCL* filters," *IEEE Trans. Ind. Electron.*, vol. 61, no. 12, pp. 6507–6516, Dec. 2014.

[38] S. Wang, J. Hu, X. Yuan, and L. Sun, "On inertial dynamics of virtual synchronous controlled based wind turbines," *IEEE Trans. Energy Convers.*, vol. 30, no. 4, pp. 1691–1702, Dec. 2015.

[39] Q.-C. Zhong, "Virtual synchronous machines: A unified interface for smart grid integration," *IEEE Power Electron. Mag.*, vol. 3, no. 4, pp. 18–27, Dec. 2016.

[40] Q.-C. Zhong and X. Zhang, "Impedance-sum stability criterion for cascaded power electronic systems," *IFAC PapersOnLine*, vol. 50, no. 1, pp. 7830–7835, 2017.

[41] F. Liu, J. Liu, H. Zhang, and D. Xue, "Stability issues of $Z + Z$ type cascade system in hybrid energy storage system (HESS)," *IEEE Trans. Power Electron.*, vol. 11, no. 29, pp. 5846–5859, Nov. 2014.

[42] P. T. Krein, J. Bentsman, R. M. Bass, and B. C. Lesieutre, "On the use of averaging for the analysis of power electronic systems," *IEEE Trans. Power Electron.*, vol. 5, no. 2, pp. 182–190, Apr. 1990.

[43] B. Lehman and R. M. Bass, "Switching frequency dependent averaged models for PWM DC-DC converters," *IEEE Trans. Power Electron.*, vol. 11, no. 1, pp. 89–98, Jan. 1996.

[44] H. K. Khalil, *Nonlinear Systems*. Prentice-Hall, 2001.

[45] L. Chua, C. Desoer, and E. Kuh, *Linear and Nonlinear Circuits*. New York, NY, USA: McGraw-Hill, 1987.

[46] W. Chen. (2002). *Introduction to Complex Analysis*. [Online]. Available: http://williamchen-mathematics.info/lnicafolder/lnica.html

[47] S. A. Saleh and M. A. Rahman, *An Introduction to Wavelet Modulated Inverters*. Hoboken, NJ, USA: Wiley, 2011.

[48] B. Wen, "Small-signal stability analysis of three-phase ac systems in the presence of constant power loads based on measured d-q frame impedances," Ph.D. dissertation, Dept. Elect. Comput. Eng., Virginia Polytech. Inst. State Univ., Blacksburg, VA, USA, 2014.

[49] X. Chen, Y. Zhang, S. Wang, J. Chen, and C. Gong, "Impedance-phased dynamic control method for grid-connected inverters in a weak grid," *IEEE Trans. Power Electron.*, vol. 1, no. 32, pp. 274–283, Jan. 2017.

[50] D. Yang, X. Ruan, and H. Wu, "Impedance shaping of the grid-connected inverter with LCL filter to improve its adaptability to the weak grid condition," *IEEE Trans. Power Electron.*, vol. 11, no. 29, pp. 5795–5805, Nov. 2014.

[51] S. M. Cuk, "Modeling, analysis, and design of switching converters," Ph.D. dissertation, Dept. Electron. Elect. Eng., California Inst. Technol., Pasadena, CA, USA, Nov. 1976.

[52] R. W. Erickson and D. Maksimov, *Fundamentals of Power Electronics*. Norwell, MA, USA: Kluwer Academic, 2001.

QING-CHANG ZHONG (M'03–SM'04–F'17) received the Ph.D. degree in control theory and engineering from Shanghai Jiao Tong University, Shanghai, China, in 2000, and the Ph.D. degree in control and power engineering from Imperial College London, London, U.K., in 2004. He is currently the Max McGraw Endowed Chair Professor of energy and power engineering with the Department of Electrical and Computer Engineering, Illinois Institute of Technology, Chicago, IL, USA, and the Founder and CEO of SYNDEM, LLC, Chicago. He proposed the synchronized and democratized (SYNDEM) grid architecture to unify the integration of millions of non-synchronous distributed generators and flexible loads based on the synchronization mechanism of synchronous machines to achieve autonomous operation of power systems.

He was a Senior Research Fellow of the Royal Academy of Engineering, U.K., and the U.K. Representative to European Control Association. He is a Fellow of IEEE and IET. He is the Vice-Chair of IFAC TC Power and Energy Systems. He serves/d as an Associate Editor for the IEEE TRANSACTIONS ON AUTOMATIC CONTROL, the IEEE TRANSACTIONS ON INDUSTRIAL ELECTRONICS, the IEEE TRANSACTIONS ON POWER ELECTRONICS, the IEEE TRANSACTIONS ON CONTROL SYSTEMS TECHNOLOGY, the IEEE ACCESS, and the IEEE JOURNAL OF EMERGING AND SELECTED TOPICS IN POWER ELECTRONICS. He is a Distinguished Lecturer of the IEEE Power Electronics Society, the IEEE Control Systems Society, and the IEEE Power and Energy Society.

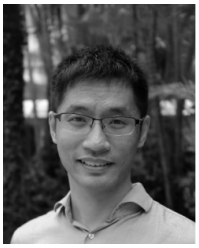

XIN ZHANG (M'15) received the Ph.D. degree in electronic and electrical engineering from the Nanjing University of Aeronautics and Astronautics, China, in 2014, and the Ph.D. degree in automatic control and systems engineering from the University of Sheffield, U.K., in 2016.

He was a Research Associate with the University of Sheffield, from 2014 to 2016, and the Postdoctoral Research Fellow with the City University of Hong Kong, in 2017. He is currently an Assistant Professor of power engineering with the School of Electrical and Electronic Engineering, Nanyang Technological University. His research interests include power electronics, power system, and advanced control theory, together with their applications in various sectors. He was a recipient of the Highly-Prestigious Chinese National Award for Outstanding Students Abroad, in 2016.